MODEL OF VORTEX FLOW OF CHARGE IN A VESSEL WITH TURBINE IMPELLER*,**

Miloslav HOŠŤÁLEK[a] and Ivan FOŘT[b]

[a] *Chemopetrol — Research Institute of Inorganic Chemistry, 400 60 Ústí nad Labem and*
[b] *Department of Chemical and Food Process Equipment Design, Czech Technical University, 166 07 Prague 6*

Received February 13th, 1986

A theoretical model is described of the mean two-dimensional flow of homogeneous charge in a flat-bottomed cylindrical tank with radial baffles and six-blade turbine disc impeller. The model starts from the concept of vorticity transport in the bulk of vortex liquid flow through the mechanism of eddy diffusion characterized by a constant value of turbulent (eddy) viscosity. The result of solution of the equation which is analogous to the Stokes simplification of equations of motion for creeping flow is the description of field of the stream function and of the axial and radial velocity components of mean flow in the whole charge. The results of modelling are compared with the experimental and theoretical data published by different authors, a good qualitative and quantitative agreement being stated. Advantage of the model proposed is a very simple schematization of the system volume necessary to introduce the boundary conditions (only the parts above the impeller plane of symmetry and below it are distinguished), the explicit character of the model with respect to the model parameters (model lucidity, low demands on the capacity of computer), and, in the end, the possibility to modify the given model by changing boundary conditions even for another agitating set-up with radially-axial character of flow.

The operation of mixing is usually realized in practice in a system illustrated in Fig. 1. It consists of a stand-up cylindrical vessel of inner diameter D_t with four symmetrically located radial baffles of width l_b. The vessel has flat bottom, and the liquid level at rest reaches height H. In the axis of the vessel there is a six-blade turbine disc impeller (Rushton type). The impeller has diameter d_m and height h, and the plane of disc occurs at the distance H_2' from the vessel bottom. By rotating the impeller at frequency n, the turbulent movement of charge is caused in which predominates the radial component of mean velocity $\langle w_r \rangle$. With increasing (radial) distance from the impeller, the portion of this component of flow turns weak (at the vessel walls reaches zero value) and, on the contrary, the proportion of axial component of mean velocity $\langle w_z \rangle$ increases. By the action of vessel walls, the liquid flow is then divided into the ascending part and the descending part, where the axial component of flow (maximum

* Part LXX in the series Studies on Mixing; Part LXIX: Collect. Czech. Chem. Commun. *52*, 1730 (1987).

** In an abridged form presented at International Conference on Mixing, Toulouse 1986

value of $\langle w_z \rangle$ in the vicinity of wall) is already quite predominant. Both the parts of flowing charge follow afterwards the system boundaries which in addition to the vessel wall consist of its bottom and the liquid level (the radial flow is again predominating), to return finally to the impeller (axial flow) and combine again in it.

When analyzing the hydrodynamics in such systems, three basic regions with different character of flow are usually delimited in the volume of agitated charge, *viz.*, the rotor region of impeller (the space circumscribed by rotating impeller), further the region of stream jet of the liquid streaking from this rotor region, and, finally, the remaining charge volume. The liquid flow immediately in the rotor region of impeller is investigated experimentally with most difficulties. Simple models assume here the existence of a so-called potential vortex with vortex core (mean velocity indirectly and/or directly proportional to radial coordinate). Both theoretically and experimentally has been best investigated the region of liquid stream jet leaving the rotor region of impeller.[1] The mean velocity profile suggests here by its course the freqency function of normal distribution with its maximum in horizontal plane of impeller symmetry. The radial profile of this maximum then represents a monotonic decreasing function of radial coordinate. The flow is here modelled with success as the discharge of submerged jet of liquid from cylindrical tangential nozzle. The results of measurement in the remaining volume of agitated charge have then only limited possibility of generalization by a form of mathematic model for they are conditioned by an actual set-up of model equipment. To make the mathematic description easier, different authors divide this remaining volume in different ways into subregions which are modelled separately with respect to the found (predominating) character of flow[2]. A disadvantage of these methods is the necessity to delimit the boundaries of the subregions, which need not be successful without

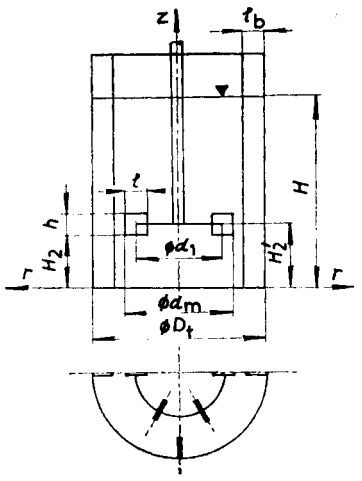

FIG. 1
Sketch of agitated system

carrying out experiments, and further the difficulties in ensuring the interconnection of single separate models. An advantage of these models, unlike the more complicated and apparently also more objective approaches based on numerical solution of respective equations of motion[3], however, is their explicit character and from it following the large lucidity of the model and easy applicability (*e.g.*, to interpolating between measured profiles).

In our paper we will concentrate upon the development of such an explicit model of mean flow of charge in system with turbine impeller and baffles which will require the dividing of the agitated charge volume only into a minimum number of further subregions. Theoretical concept of turbulent flow will be then analogous to the model of creeping flow under laminar flow regime, the transport of turbulent vorticity being analogous to the diffusion spreading of vorticity in case of laminar flow. This concept has been applied with success in case of axial high-speed impellers[4,5].

THEORETICAL

In the model system according to Fig. 1, we shall assume the fulfilment of the following simplifying presuppositions:

(1) The charge is a homogeneous Newtonian liquid,
(2) the process is isothermal and quasistationary,
(3) the mean flow is axisymmetric, the liquid stream discharging from the impeller is symmetric with respect to the horizontal plane of impeller disc,
(4) the turbulence intensity is high, the flow may be considered as fully turbulent,
(5) the vorticity transport takes place mostly by the eddy diffusion mechanism,
(6) the shape of liquid level is not influenced by its motion,
(7) the dimensions of laminar sublayer at the interface of liquid–system boundaries may be neglected.

Analogously to the Stokes simplifications of equations of motion for the creeping laminar flow[6] we can write also for our case

$$\mathbf{E}^2(\mathbf{E}^2\langle\psi\rangle) = 0\,, \tag{1}$$

where the linear differential operator $\mathbf{E}^2$ takes in cylindrical coordinates the form

$$\mathbf{E}^2 = \frac{\partial^2}{\partial r^2} - \frac{1}{r}\frac{\partial}{\partial r} + \frac{\partial^2}{\partial z^2}\,. \tag{2}$$

The stream function $\langle\psi\rangle$ is for mean flow defined by the relations

$$\langle w_r\rangle = \frac{1}{r}\frac{\partial\langle\psi\rangle}{\partial z}\,, \quad \langle w_z\rangle = -\frac{1}{r}\frac{\partial\langle\psi\rangle}{\partial r}\,. \tag{3}$$

The boundary conditions of the model are summarized in Fig. 2.

Here we have illustrated in axial cross section the boundaries of the model agitated system represented by the system axis, liquid level, bottom, and wall of agitated vessel. An additionally introduced boundary plane is the horizontal axis of symmetry of the given turbine impeller which divides the sytem into two parts: The region V_I under this plane of symmetry and further the region V_{II} which lies above it. The basic property of all the boundary surfaces is that they are not passed through with the liquid (both the regions are then, from the point of view of mass, closed systems) and the stream function $\langle\psi\rangle$ reaches a constant (zero) value on them. With the exception of the separating plane of symmetry of impeller, we do not know the tan-

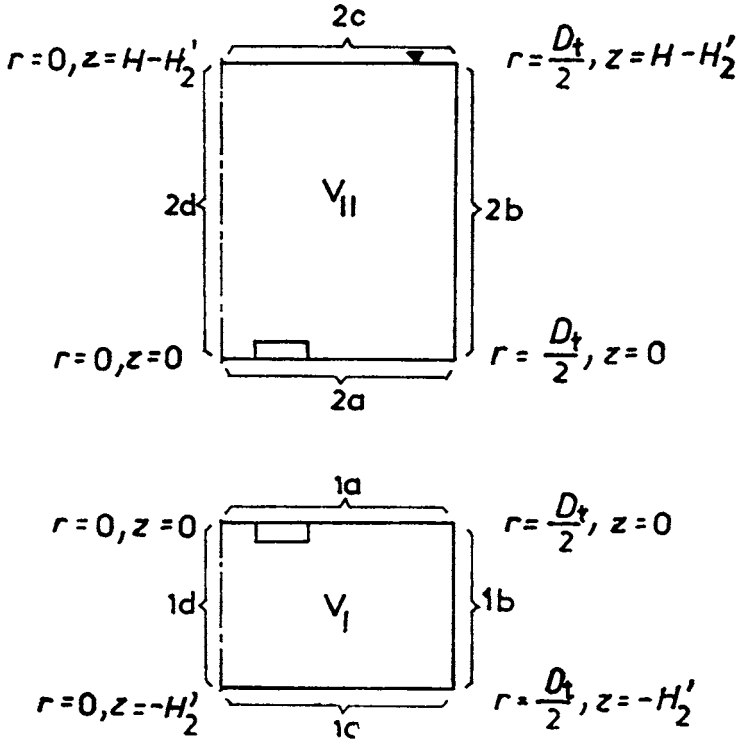

FIG. 2

Regions of modelling and boundary conditions of model. Boundary conditions of region V_I: 1a horizontal plane of impeller symmetry ($\langle\psi\rangle = 0$, $\langle w_r\rangle \geqq 0$), 1b vessel wall ($\langle\psi\rangle = 0$, $\partial\langle w_z\rangle/\partial r = 0$), 1c vessel bottom ($\langle\psi\rangle = 0$, $\partial\langle w_r\rangle/\partial z = 0$), 1d system axis ($\langle\psi\rangle = 0$, $\partial\langle w_z\rangle/\partial r = 0$). Boundary conditions of region V_{II}: 2a horiziontal plane of impeller symmetry ($\langle\psi\rangle = 0$, $\langle w_r\rangle \geqq 0$), 2b vessel wall ($\langle\psi\rangle = 0$, $\partial\langle w_z\rangle/\partial r = 0$), 2c liquid level ($\langle\psi\rangle = 0$, $\partial\langle w_r\rangle/\partial z = 0$), 2d system axis ($\langle\psi\rangle = 0$, $\partial\langle w_z\rangle/\partial r = 0$)

gential component of velocity of liquid flow, and therefore we content ourselves here for our model with introducing a zero gradient of velocity. The knowledge of radial profile of the tangent (radial) component of mean velocity is therefore assumed only on the impeller plane of symmetry which is, from the given boundaries, the only one accessible to direct experimental investigation (at least in its major part). The course of this profile is qualitatively illustrated in Fig. 3. In more detail we shall deal with in the part devoted to the model use.

Up to now we have not treated the question of the origin of coordinates and the orientation of axial coordinate z. In usual approach, the origin of coordinates is located to the point of intersection of the vessel axis with the bottom plane, the positive sense of z being considered towards the liquid level. However, to simplify at the utmost the formalism of the model solution, the origin of coordinates will be located into the horizontal plane of impeller symmetry (the orientation of z axis will be retained). Since both the modelled regions have the same boundary conditions and differ practically only in the range of axial coordinate, the solution of model equations will be carried out just for one of them (region V_{II}), and it will be outlined only how to apply the model to the remaining part of the system (region V_I).

The solution of Eq. (*1*) can be divided into two steps. If we introduce an auxiliary function $\langle\omega\rangle$, the starting differential equation of fourth order can be divided into two equations of the second order

$$\mathbf{E}^2\langle\omega\rangle = 0\,, \quad \mathbf{E}^2\langle\psi\rangle = \langle\omega\rangle\,. \tag{4a,b}$$

By using the method of separation of variables, we can find a (particular) solution of Eq. (*4a*) in the form

$$\langle\omega\rangle = 2k^2 r[\mathrm{J}_1(kr) + A\,\mathrm{N}_1(kr)]\,[D\cosh(kz) + E\sinh(kz)]\,, \quad k > 0\,, \tag{5a}$$

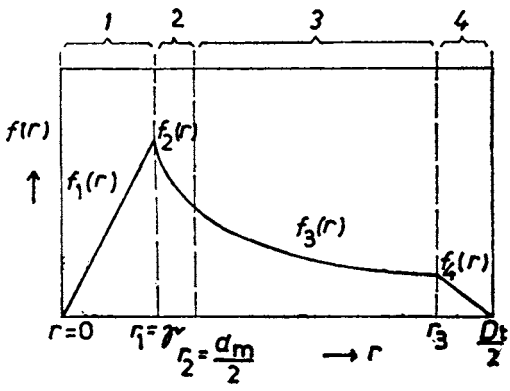

FIG. 3

Sketch of the introduction of boundary conditions in horizontal plane of impeller symmetry ($z = 0$), $f_1(r)$ relation (*15a*), $f_2(r)$ relation (*15b*), $f_3(r)$ relation (*15c*), $f_4(r)$ relation (*15d*). *1* Vortex core, *2* potential vortex, *3* submerged jet, *4* model complementation

where A, D, and E are the integration constants and k is the eigenvalue (characteristics) of the problem. Providing that we admit also the solution for $k = 0$, then the expression

$$\langle \omega \rangle = r\left(r + \frac{a}{r}\right)(2d + 6ez) \tag{5b}$$

is also the solution of Eq. (*4a*), where a, d, e are the integration constants as well. By using the method of variation of parameters, the (particular) solution of inhomogeneous equation (*4b*) is found which takes the form

$$\langle \psi \rangle = r[J_1(kr) + A\, N_1(kr)]\,\{B \cosh(kz) + C \sinh(kz) + Dkz \sinh(kz) + E[kz \cosh(kz) - \sinh(kz)]\}\,, \quad k > 0 \tag{6a}$$

and/or

$$\langle \psi \rangle = r\left(r + \frac{a}{r}\right)(b + cz + dz^2 + ez^3)\,. \tag{6b}$$

In this way we have found out the form of equation describing the mean flow of charge under the accepted simplifying conditions. Now it is necessary to confront this solution with boundary conditions of the model system.

Let us consider first a simpler form of solution (*6b*). By means of the boundary conditions in Fig. 2, we find out easily that

$$a, b, c, d, e = 0\,; \tag{7}$$

when describing the flow in a closed region, this solution consequently does not apply. It will be mentioned more closely in the discussion on the model given. Now to another variant of solution (*6a*). If we apply to it homogeneous boundary conditions for function $\langle \psi \rangle$ in axis of the vessel and at its wall, we find out that

$$A = 0 \tag{8a}$$

and

$$k_i = \lambda_i \frac{2}{D_t}\,, \quad i = 1, 2, 3, \ldots \tag{8b}$$

(here λ_i is the i-th zero point of transcendent function J_1). It follows from the last written condition (*8b*) that a general solution of our problem (*1*) will include the infinite sequence of solutions (*6a*), *i.e.*

$$\langle \psi \rangle = \sum_{i=1}^{\infty} \langle \psi_i \rangle\,, \tag{9}$$

and we must separately determine the values of remaining integration constants B, C, D, and E for each term. To be able to carry out this, we must beforehand transform in a suitable way the inhomogeneous boundary condition represented by radial profile $\langle w_r \rangle$ in the impeller plane (algebraic function $f(r)$ of radial coordinate with a finite number of terms). This is ensured by using the Fourier–Bessel expansion[7]

$$f(r) = \sum_{i=1}^{\infty} J_1\left(2\lambda_i \frac{r}{D_t}\right) F_i , \tag{10a}$$

the coefficients of this series being found in terms of the expression

$$F_i = \frac{\int_0^{D_t/2} r f(r)\, J_1\left(2\lambda_i \frac{r}{D_t}\right) \mathrm{d}r}{\int_0^{D_t/2} r J_1^2\left(2\lambda_i \frac{r}{D_t}\right) \mathrm{d}r} . \tag{10b}$$

Solution (9) satisfies the boundary conditions for the horizontal plane of the impeller symmetry ($z = 0$) if we put

$$B_i = 0 \tag{11a}$$

and

$$C_i = \frac{D_t}{2\lambda_i} F_i . \tag{11b}$$

On the remaining horizontal boundary surfaces (vessel bottom for region V_I and/or liquid level for region V_{II}), the boundary conditions are satisfied so that

$$D_i = -\frac{D_t \sinh^2\left(2\lambda_i \frac{\xi}{D_t}\right)}{2\lambda_i\left[\sinh\left(2\lambda_i \frac{\xi}{D_t}\right)\cosh\left(2\lambda_i \frac{\xi}{D_t}\right) - 2\lambda_i \frac{\xi}{D_t}\right]} F_i \tag{12a}$$

and

$$E_i = -\frac{D_t \sinh\left(2\lambda_i \frac{\xi}{D_t}\right)\cosh\left(2\lambda_i \frac{\xi}{D_t}\right)}{2\lambda_i\left[\sinh\left(2\lambda_i \frac{\xi}{D_t}\right)\cosh\left(2\lambda_i \frac{\xi}{D_t}\right) - 2\lambda_i \frac{\xi}{D_t}\right]} F_i , \tag{12b}$$

the axial coordinate of these areas taking the value

$$\xi = \begin{cases} H - H_2' & \text{(for region } V_{II}\text{)}, \\ -H_2' & \text{(for region } V_I\text{)}. \end{cases} \tag{12c}$$

Now we are already able to sum up the solution of Eq. (*1*) for conditions according to Fig. 2, into the resulting relation

$$\langle \psi \rangle (r, z) = \sum_{i=1}^{\infty} r \, J_1\left(2\lambda_i \frac{r}{D_t}\right) \frac{D_t}{2\lambda_i} F_i \left[\sinh\left(2\lambda_i \frac{z}{D_t}\right) + \sinh\left(2\lambda_i \frac{\xi}{D_t}\right) . \right.$$

$$\left. . \frac{2\lambda_i \frac{z}{D_t} \cosh\left(2\lambda_i \frac{\xi - z}{D_t}\right) - \cosh\left(2\lambda_i \frac{\xi}{D_t}\right) \sinh\left(2\lambda_i \frac{z}{D_t}\right)}{\sinh\left(2\lambda_i \frac{\xi}{D_t}\right) \cosh\left(2\lambda_i \frac{\xi}{D_t}\right) - 2\lambda_i \frac{\xi}{D_t}} \right] . \tag{13a}$$

Furthermore, allowing for definition relations (*3*), we derive easily further relations for calculating the mean velocity components, namely

$$\langle w_r \rangle (r, z) = \sum_{i=1}^{\infty} J_1\left(2\lambda_i \frac{r}{D_t}\right) F_i \left[\cosh\left(2\lambda_i \frac{z}{D_t}\right) - \sinh\left(2\lambda_i \frac{\xi}{D_t}\right) . \right.$$

$$\left. . \frac{2\lambda_i \frac{z}{D_t} \sinh\left(2\lambda_i \frac{\xi - z}{D_t}\right) - \cosh\left(2\lambda_i \frac{\xi - z}{D_t}\right) + \cosh\left(2\lambda_i \frac{\xi}{D_t}\right) \cosh\left(2\lambda_i \frac{z}{D_t}\right)}{\sinh\left(2\lambda_i \frac{\xi}{D_t}\right) \cosh\left(2\lambda_i \frac{\xi}{D_t}\right) - 2\lambda_i \frac{\xi}{D_t}} \right] \tag{13b}$$

and/or

$$\langle w_z \rangle (r, z) = -\sum_{i=1}^{\infty} J_0\left(2\lambda_i \frac{r}{D_t}\right) F_i \left[\sinh\left(2\lambda_i \frac{z}{D_t}\right) + \sinh\left(2\lambda_i \frac{\xi}{D_t}\right) . \right.$$

$$\left. . \frac{2\lambda_i \frac{z}{D_t} \cosh\left(2\lambda_i \frac{\xi - z}{D_t}\right) - \cosh\left(2\lambda_i \frac{\xi}{D_t}\right) \sinh\left(2\lambda_i \frac{z}{D_t}\right)}{\sinh\left(2\lambda_i \frac{\xi}{D_t}\right) \cosh\left(2\lambda_i \frac{\xi}{D_t}\right) - 2\lambda_i \frac{\xi}{D_t}} \right] . \tag{13c}$$

Use of Model

To verify our model, we have chosen the set-up of the agitated system according to Fig. 1 which is summarized in Table I. In this configuration, the horizontal plane of the impeller symmetry divides the space of agitated system so that the volume of region V_{II} is nearly twice compared to region V_I. The boundary conditions in the plane of impeller $z = 0$ are based on equations which for the liquid stream leaving impeller have been reported by Drbohlav and coworkers[1], *i.e.*,

$$\langle \psi \rangle = \alpha \left(\frac{r}{\beta}\right)^{1/2} (r^2 - \gamma^2)^{1/4} \operatorname{tgh}\left(\beta \frac{z}{2r}\right), \tag{14a}$$

$$\langle w_r \rangle = \frac{\alpha}{2} \left(\frac{\beta}{r^3}\right)^{1/2} (r^2 - \gamma^2)^{1/4} \left[1 - \operatorname{tgh}^2\left(\beta \frac{z}{2r}\right)\right], \tag{14b}$$

the parameters α, β, γ taking the following values

$$\alpha = 0{\cdot}70 n d_m\,, \quad \beta = 11{\cdot}2\,, \quad \gamma = 0{\cdot}68\,(d_m/2)\,. \tag{14c}$$

By inserting the value $z = 0$ into relations (*14*), we get the boundary conditions corresponding to part 3 of the curve in Fig. 3. The other parts of profile $f(r) = \langle w_r \rangle (r, z = 0)$ are then complemented so as to obtain a continuous curve and simultaneously to fulfil the boundary conditions for $r = 0$ or $r = D_t/2$. In this way we obtain the following relations:

Direct proportionality for the vortex core (part *1*)

$$f_1(r) = \frac{\alpha}{2} \left(8 \frac{\beta}{d_m^3}\right)^{1/2} \left(\frac{d_m^2}{4} - \gamma^2\right)^{1/4} \frac{d_m}{2\gamma^2} r\,, \quad r \in \langle r = 0; r_1 = \gamma \rangle\,, \tag{15a}$$

hyperbolic dependence for a potential vortex (part 2)

$$f_2(r) = \frac{\alpha}{2} \left(8 \frac{\beta}{d_m^3}\right)^{1/2} \left(\frac{d_m^2}{4} - \gamma^2\right)^{1/4} \frac{d_m}{2} \frac{1}{r}\,, \quad r \in \left\langle r_1 = \gamma; r_2 = \frac{d_m}{2} \right\rangle, \tag{15b}$$

TABLE I

Arrangement of the agitated system chosen to verify the model (see Fig. 1)

H/D_t	H_2/D_t	H_2'/D_t	l_b/D_t	d_m/D_t	d_1/d_m	l/d_m	h/d_m
1	1/3	0·367	0·1	1/3	0·75	0·25	0·2

for submerged liquid jet (part 3)

$$f_3(r) = \frac{\alpha}{2}\left(\frac{\beta}{r^3}\right)^{1/2}(r^2 - \gamma^2)^{1/4}, \quad r \in \left\langle r_2 = \frac{d_m}{2}; r_3 < \frac{D_t}{2}\right\rangle, \tag{15c}$$

complementation of the remaining part of profile by a straight line (part 4)

$$f_4(r) = \frac{\alpha}{2}\left(\frac{\beta}{r_3^2}\right)^{1/2}(r_3^2 - \gamma^2)^{1/4}\left[\frac{(D_t/2) - r}{(D_t/2) - r_3}\right], \quad r \in \left\langle r_3 \gg \frac{d_m}{2}, r_4 = \frac{D_t}{2}\right\rangle. \tag{15d}$$

Thus, the boundary between the 1st and 2nd part of profile $f(r)$ has been defined identically with the radius of cylindrical tangential jet γ. Boundary r_3 has then been defined (an estimate) in the distance of $l_b/2$ from the vessel wall ($r_3 = (D_t - l_b)/2$).

Integral in the numerator of relation (*10b*) must be written out, on applying these conditions, in the following way:

$$\int_0^{D_t/2} rf(r)\, J_1\left(2\lambda_i \frac{r}{D_t}\right) dr = \sum_{j=1}^{m} \int_{r_{j-1}}^{r_j} rf_j(r)\, J_1\left(2\lambda_i \frac{r}{D_t}\right) dr, \tag{16a}$$

where m is in this case equal 4. To prevent difficulties in integration, the situation has been further simplified before the calculation itself by approximating the originally nonlinear parts of profile (*15b*), (*15c*) by one and/or four straight-line sections of the type

$$f_k \doteq p_k r + q_k, \quad k = 2, 3a, 3b, 3c, 3 \tag{16b}$$

and solving expression (*16a*) for 7 straight-line sections of profile $f(r)$.

RESULTS AND DISCUSSION

When performing the calculations according to the given model, it is impossible, for the obvious reasons, to work with infinite number of terms in sequences (*9*)–(*13*). To put it otherwise, the applicability of the obtained solution of equation of motion (*1*) is conditioned by a rapid convergence of these series to the solution sought. Further we shall get acquainted with the results which have been obtained on using a minicomputer WANG 2200.

In Fig. 4 the course of the bounary condition of $f(r)$ as approximated by seven interconnected straight-line sections (broken line) in comparison with the results of replacement of this profile (solid line) by means of sequence (*10*). It can be seen that the above-mentioned series renders the initial function $f(r)$ comparatively closely already on using the first four terms. After further increase in the number

of terms to double, the error of approximation of the original (in sections straight--line) dependence by series (*10*) may be considered as quite inferior. The parameters of this series are then summarized in Table II. Thus, with increasing number of employed terms of the theoretical solution, we reach first preciser results, however, with increasing values of parameter k_i, the problems of numerical nature gradually grow – the rounding-off error manifests itself still more strongly, and, finally, the error of overflow or underflow of numerical data may appear (with the minicomputer WANG 2200, the admissible range is 10^{-99} to 10^{99}). For the purposes of this paper, we shall hereinafter work with the first five terms of solution of Eq. (*1*).

TABLE II

Result of the application of boundary conditions of the model

i	K_i/D_t^{-1}	F_i/nd_m
1	7·66341	3·31403
2	14·03117	0·89204
3	20·34693	1·58085
4	26·64738	0·12088
5	32·94126	0·42119
6	39·23171	−0·43981
7	45·52016	−0·16055
8	51·80734	−0·35296

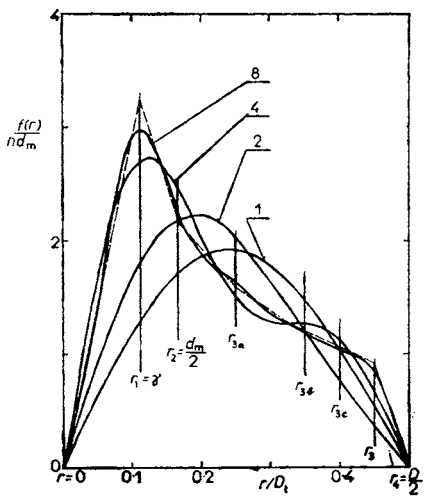

FIG. 4

Comparison of the course of boundary condition $f(r)$ in the form of straight lines in parts (broken line) with the result of $f(r)$ expansion into the Fourier–Bessel series for different number (1, 2, 4, and 8) of terms of this series

To verify the correctness of the model presented, the model by Drbohlav and coworkers[1] can again serve, which has already been used when introducing the boundary conditions in the horizontal plane of impeller symmetry ($z = 0$). The result of comparison of axial profiles $\langle w_r \rangle$ and $\langle \psi \rangle$ for region V_{II} is illustrated in Figs 5 and 6. It follows from Fig. 5 that in the liquid stream streaking from the rotor region ($r = d_m/2$, $z \in \langle 0, h/2 \rangle$), the model presented exhibits a gentler course of quantity $\langle w_r \rangle$ than the model by Drbohlav and coworkers[1] but the difference in the stream function values according to both models is here lower than 10%. Considering that the model presented specifies in no way the axial dimensions of the rotor region, this agreement is surprisingly good. In the next part of profile ($z > h/2$) we cannot any more rely upon the model by Drbohlav and coworkers[1] because this part occurs outside the region of liquid stream out of impeller. Further comparison of both the models is made possible in Fig. 6. The value of radial coordinate has been chosen so that the axial profile $\langle \psi \rangle$ in agreement with the model presented

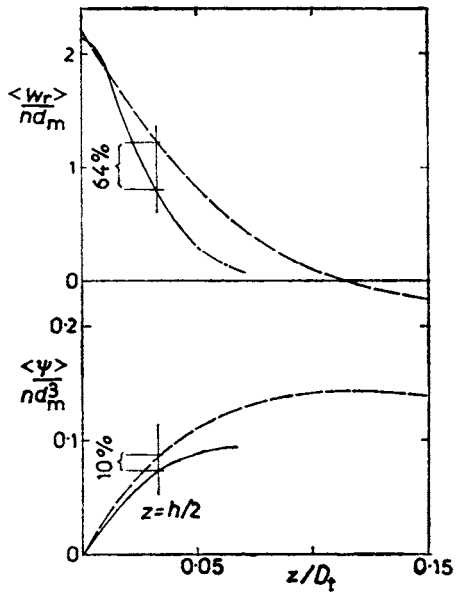

FIG. 5

Comparison of results of the calculation of axial profile of quantities $\langle w_r \rangle$ and $\langle \psi \rangle$ (region V_{II}, $r = d_m/2$) at the stream from rotor region (broken line — model presented, solid line — work by Drbohlav and coworkers[1])

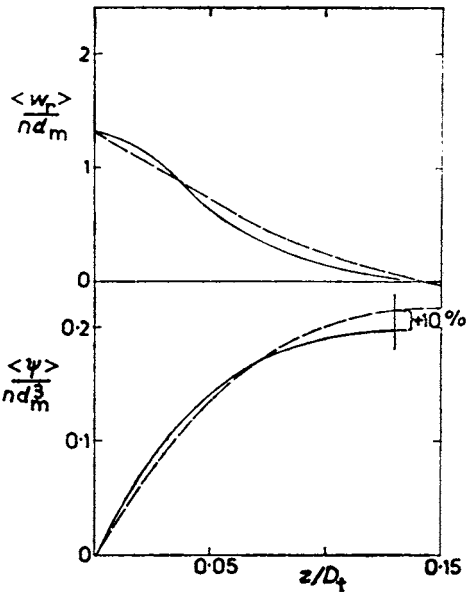

FIG. 6

Comparison of results of the calculation of axial profile of quantities $\langle w_r \rangle$ and $\langle \psi \rangle$ in the region V_{II} for $r/D_t = 0{\cdot}31$ (broken line — model presented, solid line — work by Drbohlav and coworkers[1])

should comprise the value of this function being maximum from the point of view of the whole agitated system ($r/D_t \doteq 0{\cdot}31$; $\langle\psi\rangle/nd_m^3 \doteq 0{\cdot}22$). Thereby, a pleasant finding is that the difference of values $\langle\psi\rangle$ unlike the results of modelling according to Drbohlav and coworkers[1] is not again higher than about 10%. The course of quantity $\langle w_r\rangle$ as well predicted by both the models exhibits a very good quantitative agreement.

Examples of radial profiles $\langle w_z\rangle$ and $\langle\psi\rangle$ are given in Fig. 7 (region V_{II}, $z/D_t = 0{\cdot}18$) and Fig. 8 (region V_I, $z/D_t = -0{\cdot}18$). The comparison of modelling (broken line) with the experimental data by Fořt and coworkers[8] (points) for a close-to-wall flow is in Fig. 7. It follows from the comparison that the model predicts a flatter velocity profile here than that given by experiments even though the liquid volumetric flow characterized by the maximum of radial profile $\langle\psi\rangle$ can be for both the cases estimated as very close. As to the descending flow in the vicinity of vessel axis, it is possible to refer to, *e.g.*, the work by Fořt, Hrach, and Obeid[9] where much flatter

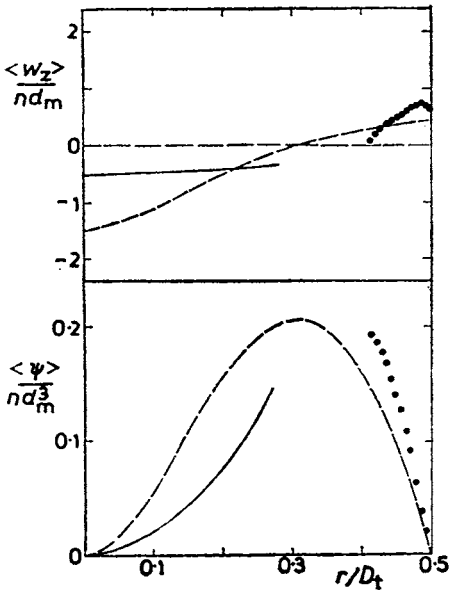

FIG. 7

Comparison of radial profile of quantities $\langle w_z\rangle$ and $\langle\psi\rangle$ (region V_{II}, $z/D_t = 0{\cdot}18$) by the model presented (broken line) with results of measurement (● data by Fořt and coworkers[8], solid line — data by Fořt and coworkers[9])

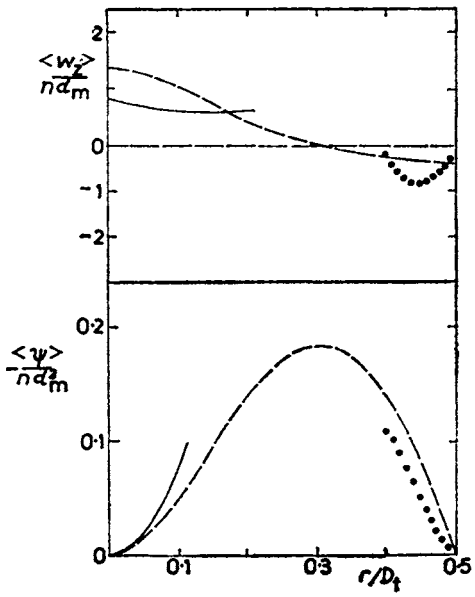

FIG. 8

Comparison of radial profile of quantities $\langle w_z\rangle$ and $\langle\psi\rangle$ (region V_I, $z/D_t = -0{\cdot}18$) by the model presented (broken line) with the results of experimental determination of $\langle\psi\rangle$ (● data by Fořt and coworkers[8], solid line — data by Fořt and coworkers[9])

profile of quantity $\langle w_z \rangle$ is reported contrary to the model presented. Similar situation may be stated in region V_I, too (see Fig. 8). Let us add to Figs 7 and 8 that the data by Fořt and coworkers[8,9] originate from experiments carried out in a vessel of small dimensions ($D_t = 0{\cdot}29$ m) whereas the work of Drbohlav and coworkers[1], among others, originates in measurements in a large vessel ($D_t = 1$ m).

The field of stream lines $\langle \psi \rangle / nd_m^3 = \text{const.}$ in agitated system, as predicted by the model presented, is illustrated in Fig. 9.

With regard to a considerable idealization of reality which has enabled us to simplify at most the initial equation of the charge vortex flow, we may consider the agreement of results of modelling with the results of other authors as good. For example, in radial flow in the direction from impeller to the vessel wall, the error of calculation, as compared with the quantitative model by Drbohlav and coworkers[1], is lower than 10%. Rather less favourable is the result of modelling of the axial velocity component in the axial flow and/or close-to-wall flow where the model presented predicts rather a steeper (for axial flow) and/or flatter (for close-to-wall flow) radial profile $\langle w_z \rangle$. The second case is thereby in relation with the 7th introduced presupposition. Even in these regions, however, it is possible to state a good agreement with data of other authors, at least as to the overall flow rate of liquid. Priority of the model presented is the simple initial dividing of the model system into two

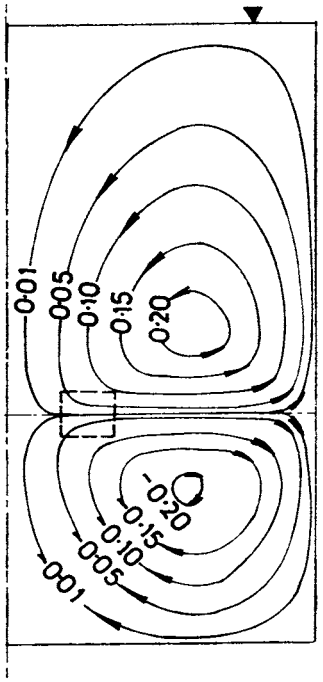

FIG. 9

Results of the calculation of streamline field $\langle \psi \rangle / nd_m^3 = \text{const.}$ in agitated system by the model presented

regions of cylindrical shape (under and above the horizontal plane of impeller symmetry). For example, it is not necessary to specially localize the axial dimensions of rotor region of impeller. This property excels especially when comparing with application of the very simple model by Fořt and coworkers[2] which, however, requires the division of system altogether to fourteen parts. The boundary conditions of solution are as well very simple. On most boundary surfaces, the homogeneous boundary conditions are namely concerned. Only on the horizontal plane of impeller symmetry, which is from greater part easily accessible to measurement, it is necessary to start from actual conditions in a system. We have particularly used here the reliable model by Drbohlav and coworkers[1] describing the whole region of discharge from the turbine impeller (the model of submerged liquid jet) which was complemented in the remaining parts of this boundary area (rotor region of impeller, close-to-wall flow) in terms of simple model concepts. This all have enabled us to obtain the solution of initial equation for the stream function $\langle\psi\rangle$ and velocity components $\langle w_r\rangle$, $\langle w_z\rangle$ in an explicit form. Despite the open form of solution (infinite series), the application of model is, however, computationally easy to manage owing to a rapid convergence of these series. Thus, for practical purpose, we shall undoubtedly be able to cope with several first (five to ten) terms of the solution. Ease to realize the calculations according to the given model is then a great advantage against the implicit models based on a more general form of initial transport equations and more realistic boundary conditions (let us name, *e.g.*, the work by Placek[3]). Thanks to substantially lower demands on a computer storage capacity, the model presented can be used more easily as a part of wider models describing further processes in agitated system which are immediately conditioned by the hydrodynamics of system. The model presented can be applied, on changing the boundary conditions, also to other arrangements of agitated system with prevailing axially-radial flow. The modelled (cylindrical) region does not have to be closed from the point of view of mass transfer. Providing that, *e.g.*, some of bases is passed through with a liquid, it is necessary, besides the radial profile $\langle w_r\rangle$, to consider also the profile $\langle w_z\rangle$ or $\langle\psi\rangle$. Liquid may also flow through some of cylindrical boundaries of the model subregion (see, *e.g.*, the division used in work[2]). In case that the total flow rate through some boundary surface is not equal zero, so-called zero terms will have an effect in solution, too; here, *e.g.*, represented by formula (*6b*). As far as constants of solution d, e and/or D, E are set equal to zero, we get a description of potential flow used, *e.g.*, in work[2] or in work[10]. In case that the profiles of quantities $\langle w_r\rangle$ (or $\langle\psi\rangle$) and $\langle w_z\rangle$ on some of cylindrical boundary areas should be regarded as boundary conditions, it would be necessary to derive the solution in terms of the procedure used in work[5], in which the problem solution was limited to the finding of the zero term only of general solution.

LIST OF SYMBOLS

A integration constant
a integration constant, m^2
B integration constant, $m^2\ s^{-1}$
b integration constant, $m\ s^{-1}$
C integration constant, $m^2\ s^{-1}$
c integration constant, s^{-1}
D integration constant, $m^2\ s^{-1}$
D_t diameter of agitated vessel, m
d integration constant, $m^{-1}\ s^{-1}$
d_m impeller diameter, m
d_1 diameter of separating disc of turbine impeller, m
E integration constant, $m^2\ s^{-1}$
$\mathbf{E}^2$ differential operator
e integration constant, $m^{-2}\ s^{-1}$
F coefficient of Fourier–Bessel expansion, $m\ s^{-1}$
$f(r)$ course of radial component $\langle w_r \rangle$ in horizontal plane of impeller symmetry, $m\ s^{-1}$
H height of liquid in agitated tank, m
H_2 distance of lower edge of impeller blades from bottom, m
H_2' distance of impeller disc from bottom, m
h height of impeller blades, m
J_ν cylindrical (Bessel) function of first kind of index ν
k characteristic number, m^{-1}
l length of impeller blade, m
l_b width of radial baffle, m
m number of sections of radial profile of function $f(r)$
N_ν cylindrical function of second kind (Neumann) of index ν
n impeller frequency of revolution, s^{-1}
p straight-line slope, s^{-1}
q straight-line absolute term, $m\ s^{-1}$
r radial coordinate, m
$\langle w \rangle$ mean velocity of liquid, $m\ s^{-1}$
z axial coordinate, m
α parameter of Eqs (*14*)
β parameter of Eqs (*14*)
γ parameter of Eqs (*14*)
ξ value of axial coordinate z, m
λ root of function J_1
$\langle \psi \rangle$ Stokes stream function for mean flow, $m^3\ s^{-1}$
$\langle \omega \rangle$ auxiliary function, $m\ s^{-1}$

Subscripts

i general summation index
j general summation index
r radial component
z axial component

Other Designation

I region below horizontal plane of impeller symmetry
II region above horizontal plane of impeller symmetry

REFERENCES

1. Drbohlav J., Fořt I., Krátký J.: Collect. Czech. Chem. Commun. *43*, 696 (1978).
2. Fořt I., Obeid A., Březina V.: Collect. Czech. Chem. Commun. *47*, 226 (1982).
3. Placek J.: *Thesis.* Czechoslovak Academy of Sciences, Prague 1980.
4. Hošťálek M., Fořt I.: Collect. Czech. Chem. Commun. *50*, 930 (1985).
5. Hošťálek M., Fořt I.: Collect. Czech. Chem. Commun. *50*, 2396 (1985).
6. Jenson V. G., Jeffreys G. V.: *Mathematical Methods in Chemical Engineering.* Academic Press, London 1963.
7. Korenev B. G.: *Vvedenie v teoriyu Besselevykh funktsii.* Nauka, Moscow 1971.
8. Fořt I., Placek J., Strek F., Jaworski Z., Karcz J.: Collect. Czech. Chem. Commun. *44*, 684 (1979).
9. Fořt I., Hrach M., Obeid A.: Sb. Vys. Sk. Chem.-Technol. Praze K *15*, 37 (1980).
10. Fořt I., Jaroch O., Hošťálek M.: Collect. Czech. Chem. Commun. *42*, 3555 (1977).

Translated by J. Linek.